Optical design concept for the Giant Magellan Telescope Multi-object Astronomical and Cosmological Spectrograph (GMACS)

Luke M. Schmidt*[a], Rafael Ribeiro[b], Keith Taylor[c], Damien Jones[d], Travis Prochaska[a], Darren L. DePoy[a], Jennifer L. Marshall[a], Erika Cook[a], Cynthia Froning[e], Tae-Geun Ji[f], Hye-In Lee[f], Claudia Mendes de Oliveira[b], Soojong Pak[f], Casey Papovich[a]

[a]Department of Physics and Astronomy, Texas A&M University, 4242 TAMU, College Station, TX, 77843-4242 USA; [b]Departamento de Astronomia, IAG, Universidade de São Paulo, Cidade Universitária, 05508-900, São Paulo, Brazil; [c]Instruments4, CA 91011, USA; [d]Prime Optics, Australia; Department of Astronomy, C1400, [e]University of Texas at Austin, Austin, TX 78712; [f]School of Space Research, Kyung Hee Univeristy, Yongin-si, Gyeonggi-do 17104, Republic of Korea

ABSTRACT

We present a preliminary conceptual optical design for GMACS, a wide field, multi-object, optical spectrograph currently being developed for the Giant Magellan Telescope (GMT). We include details of the optical design requirements derived from the instrument scientific and technical objectives and demonstrate how these requirements are met by the current design. Detector specifications, field acquisition/alignment optics, and optical considerations for the active flexure control system are also discussed.

Keywords: GMT, Extremely Large Telescopes, spectrograph, multi-object spectrograph, optical instruments

1 INTRODUCTION

The Giant Magellan Telescope Multi-object Astronomical and Cosmological Spectrograph (GMACS) is a first light instrument for the Giant Magellan Telescope (GMT). It will provide wide field, multi-object, moderate resolution spectroscopy of faint targets, currently only known from imaging observations. The new optical design concept for the GMACS double-beam optical spectrograph consists of a common pan-chromatic collimator, a dichroic beam-splitter, a set of volume-phase holographic transmission gratings (VPHGs) as the dispersion elements, a set of passband filters for both direct imaging and spectroscopic waveband selection, feeding twin red and blue optimized *f*/2.2 CCD cameras.

The collimator generates an image of the telescope entrance pupil, located at its primary (sparse aperture) mirror, onto the optical center of the VPHG. The pupil aberrations must be well corrected due to the strong astigmatism and field curvature caused by the telescope to avoid overloading the corrections needed by the cameras. The convex radius of curvature of the telescope focal plane is ~2200mm formed at *f*/8.16 giving an image diameter of ~450 mm for a 7.5 arcminute field of view (FoV).

The proposed optical designs described in this paper are analyzed for both direct imaging and low and high resolution spectroscopy for the most demanding blue arm.

A previous 4-shooter, ultra-wide field concept for GMACS was developed in 2011 which employed a tent mirror placed after a field lens to divide the incident focal plane into four separate segments to avoid physical interference between the multiple fly's eye collimators[1]. These four fold mirrors at the GMT focal plane redirected a 9 arcminute × 18 arcminute FoV to four individual arms that each comprised a double-beam spectrograph (that is, each arm saw a 4.5 × 9 arcminute off-axis field). However, despite the good performance achieved with this off-axis concept, the complexity and cost necessitated a de-scope to a single on-axis double-beam version. Nevertheless, several optomechanical concepts were migrated to the new design.

We have chosen to begin the study of the GMACS optical design with the blue camera due to the challenging requirement for high throughput in the UV-blue region which aims for significant throughput down to 320nm. The necessity for large lenses coupled with the requirement for high internal glass transmittance limits glass choices from

* lschmidt@physics.tamu.edu; phone 1-979-845-4401; http://instrumentation.tamu.edu

optical suppliers. The lessons learned in the blue camera design will be used in the design of the red camera that will be studied during the conceptual design phase. Additional GMACS design information can be found in the overview (9908-79)[2] and optomechanical (9908-375)[3] papers, also at this conference.

2 REQUIREMENTS

Through collaboration with the Giant Magellan Telescope Organization (GMTO), its partners and other representatives from the scientific community, a set of principal functional requirements has been developed (Table 1). A 2014 GMACS community workshop included more than 50 participants with interests in a broad range of research topics including (1) stars, star-formation, and planets; (2) resolved galaxies (including dwarf galaxies) and near-field cosmology; and (3) distant galaxies (including reionization and first light science).

Additional performance goals and practical constraints also guide the design. For example, throughput is an important design driver. The throughput requirements and goals for GMACS are:

> **Requirement:** 350-950nm, peak transmission ≥40%, no worse than 25% of peak at any wavelength. 320-350nm and 950-1040nm, best effort, no design choices to preclude transmission.
>
> **Goal:** 320-1000nm with peak transmission ≥40%, no worse than 25% of peak at any wavelength. Transmission beyond 1000nm, best effort, no design choices to preclude transmission to red sensitivity limit of the CCD.

These throughput requirements take into consideration the telescope throughput, grating efficiency and detector quantum efficiency. However, in this paper we discuss the throughput considering only the GMACS optical system.

GMACS must also interface with MANIFEST, the GMT fiber positioner[4]. GMACS must have sufficient optical performance to take advantage of the reduced slit width of the fiber output that will allow higher resolution observations with the combined GMACS-MANIFEST system.

GMACS is designed for the Direct Gregorian Narrow-Field (DGNF) configuration of the GMT. The instrument mounts at the focus of the primary/secondary mirror system and does not include an atmospheric dispersion compensator, wide field corrector or any fold mirrors. Uncorrected image quality places an upper limit of ~5 arcminutes for the radius of the field of view.

Table 1 GMACS Principal Functional Parameters

Parameter	Requirement	Goal
Field of View	30 arcmin sq.	50 arcmin sq.
Wavelength Coverage	350-950nm	320-1000nm
Spectral Resolution	Blue: 1000-6000, Red 1000-6000	Blue: 1000-6000, Red 1000-6000
Image Quality	80% EE at 0.30 arcsec	80% EE at 0.15 arcsec
Spectral Stability	0.3 spectral resolution elements/hour	0.1 spectral resolution elements/hour
Number of Gratings	2	≥2
Slit Mask Exchange	12	≥20

3 OPTICAL DESIGN

3.1 Design Methodology

Prior to the detailed optical design process, a functional parameter study was performed. Using the stated requirements and the optical design of the GMT a range of possible spectrograph parameters were determined. This included the number of pixels (15μm) along a slit that covers the full diameter of the FoV, different aspect ratios for the detector, and requirements for collimator focal length, pupil diameter and camera focal length. The camera FoV required to capture a continuous spectrum at the desired resolutions was also determined. Difficulties in designing and building very fast

cameras (~*f*/1) or wide FoV cameras, as well as physical constraints on pupil (and therefore grating) size determined the starting point for the design presented here.

The design methodology used in this paper was based on independent optimization of the collimator and camera, described below. Once the basic optical parameters (effective focal length, waveband coverage, FoV) had been established for the collimator optical system, early variants of the system were optimized using Zemax™. Three flat windows which represent the dichroic, VPHG and filter are included in the prescription of the collimator with the location of the first and second determined by the space required for their rotation. A paraxial surface was then inserted to simulate the camera.

For the camera, the stop diameter and position of the system are given by the exit pupil properties of the collimator. The pupil space is chosen to permit space for the dichroic and VPHG. The camera FoV is based on the grating dispersion and wavelength coverage and ultimately limited by the chosen format of the detector.

Finally, both the collimator and camera are brought together into the same Zemax™ prescription to allow fine tuning of the optimization taking into account different grating configurations.

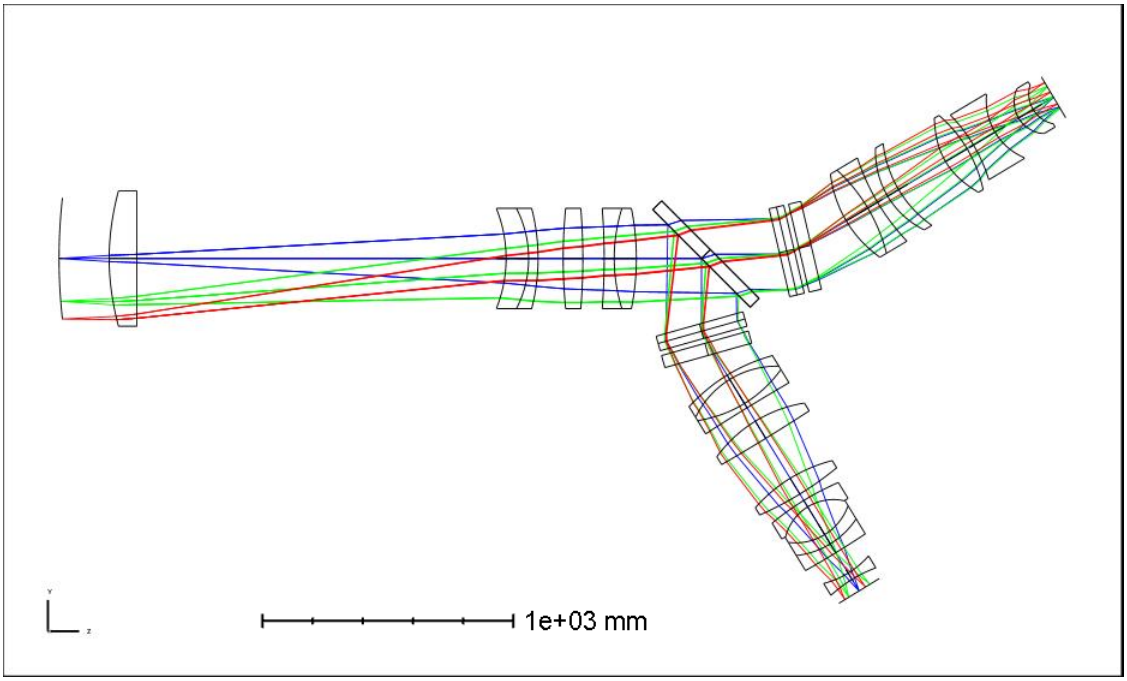

Figure 1. GMACS optical layout. Light from the telescope enters from the left. A beamsplitter separates the light into red (transmitted) and blue (reflected) channels. The red camera is included to convey the overall design concept while this paper focuses on the development of the broadband collimator and blue camera.

3.2 System Overview

The principal functional parameters of the system are summarized in the table below:

Table 2. Current system parameters for the collimator and UV-blue camera.

Basic System Parameters	
On axis telescope focal plane to CCD image plane	3920mm
Focal lengths	System: 5946.3mm Collimator: 2200mm UV-Blue Camera: 592mm
System working *f*-number	2.19
Telescope primary mirror (entrance pupil diameter)	25448 mm

Collimator exit pupil diameter	270 mm
Wavelength coverage (requirement)	340 – 580nm
Detector Format	2-by-3 4k², 15µm (8k-by-12k) pixel CCD (or 122.8 by 184.3mm) with long dimension in the dispersion direction.
Camera Field of view (diameter)	14°
Lens system:	
Number of elements	**Collimator**: 6 elements (2 singlets and 2 doublets) **UV-Blue Camera**: 10 elements (1 quadruplet, 1 triplet and 3 singlets) 1 Dichroic and 3 VPHG (low, med, high resolution)
Glasses	Fused Silica, FPL51, BSM51Y, BAL35Y, PSK3, CaF_2, FK54
Aspheric surfaces	Collimator: 1 UV-Blue Camera: 3
Coatings	Quarter wave of MgF_2 coating for lenses and silver for telescope primary and secondary mirror. The influence on the throughput was mainly a function of the internal absorption of the glasses. No detailed spectral and angular transmittance was included in the beamsplitter and the grating efficiency was considered perfect. Future calculations will update mirror and lens coatings, and grating throughput to match expected performance.
Packaging:	
BFD (last camera surface to CCD)	≈ 34mm (center) ≈ 20mm (edge)
Maximum lens diameter	≈ 580mm (Fused Silica Field Lens)
Lens Weight	270 kg, based on the volume and density of Zemax™ data base glasses properties

In the sections below we describe the subsystems of the GMACS blue arm optical system which comprises the collimator and camera.

3.3 Collimator

The current design of the collimator consists of four elements: a silica field lens immediately behind the telescope focus; two doublets and a singlet, which reimage the telescope aperture onto the central plane of the VPHG. The collimator produces a 270mm diameter exit pupil approximately 520mm beyond the vertex of the last lens.

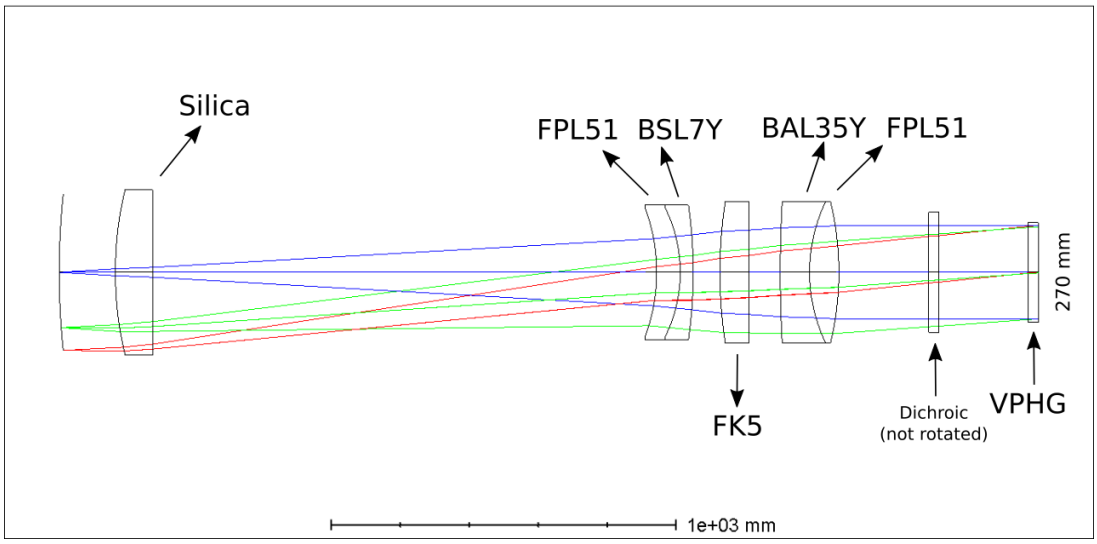

Figure 2. Collimator optical layout

3.4 Blue Camera

Several different optical concepts for the blue camera were explored to determine which had the best promise of meeting the image quality requirements. Included among these were the Sonnar and Petzval concepts with an adaption of the latter presented here. The necessary solution differs from the common Petzval camera resulting from the fact that the entrance pupil is located relatively far from the first lens in order to allow for VPHG rotation. It is analogous to a long "eye relief" requirement for an eyepiece design with the consequence that larger optical elements are required.

The original motivation for using a Sonnar concept in the earlier GMACS camera design was that it allowed for variations in camera f-numbers with relatively few modifications to the basic optical configuration. For instance, a faster camera would decrease the detector size and conserve the same field of view. However, although the overall performance was considered acceptable, the highly powered elements required the system to have tight surfaces and assembly tolerances. For this reason, we chose to study a Petzval adaptation.

The basic Petzval optical system consists of two positive elements spaced apart, usually achromatic doublets or triplets. It produces a large Petzval curvature requiring a strong negative field flattener placed close to the focal plane. In this context the field flattener has little effect on the focal length or aberration balance, but does allow a correction to the Petzval field curvature and, in special cases, the distortion. However, the field flattener has some drawbacks; for example, in order to correct the Petzval field curvature the working distance of the system is decreased, which can generate stray light and undesirable imaging of its surface defects[5].

The blue camera layout is illustrated in Figure 3 below. In imaging mode, this *f*/2.2 camera creates a 0.3 arcsec RMS image over a ~7.5 arcmin FoV, equivalent to a 14° field.

The space between the FK54 and FPL51 singlets is required to accommodate a shutter mechanism. The back focal distance of the camera is 34 mm at the vertex of the last surface and the optical axis. For the next iterations of the camera design, we will explore the effects of replacing the last concave surface of the field flattener with a planar or convex surface in order to reduce stray light and ghost reflection contamination.

We shall also be studying an alternative camera concept based on an ~*f*/1 catadioptric camera, which is briefly discussed in Section 7. Although this solution would bring new possibilities for the blue arm related to high UV throughput, our current main objective is to achieve a reasonable GMACS design which meets the Table 1 requirements.

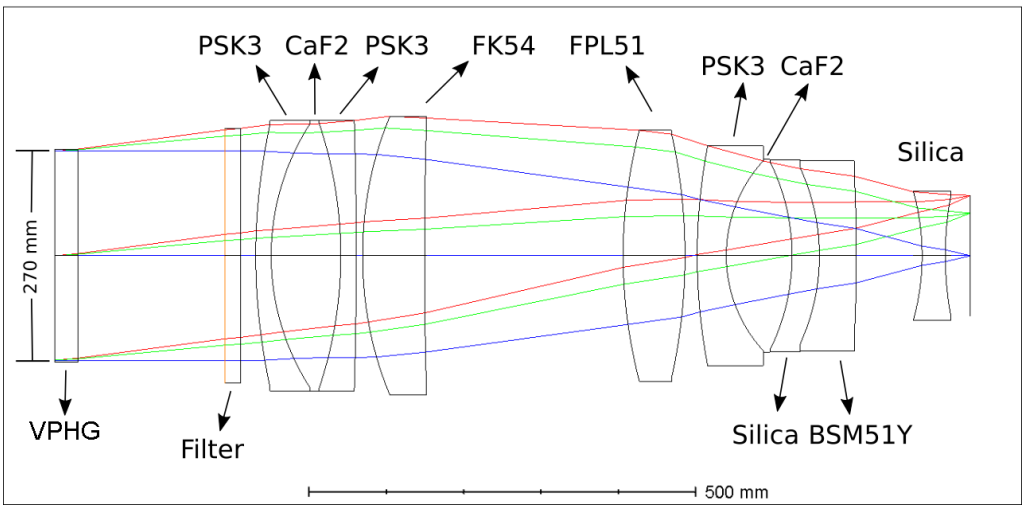

Figure 3. Blue camera in imaging mode

3.5 Detector

The detector assembly will be formed by a 2-by-3 mosaic of 4096 × 4096 detectors with a pixel pitch of 15µm. If the camera designs evolve to faster focal ratios, we may consider a 1-by-2 mosaic of $6k^2$ detectors, also with a pixel pitch of 15µm. When accounting for the necessary gap between devices, this would increase the fill factor from 91% to 98%. It would also be possible to use a 2-by-2 mosaic of $6k^2$ detectors, but with the current design, 4k of "spatial" pixels would be outside the FoV. We are investigating modification of existing devices to one-sided readout, which reduces the gap in the spatial dimension.

Below are an illustration of the 2-by-3 mosaic of $4k^2$ detectors mosaic detectors and a table which summarizes the sensor parameters:

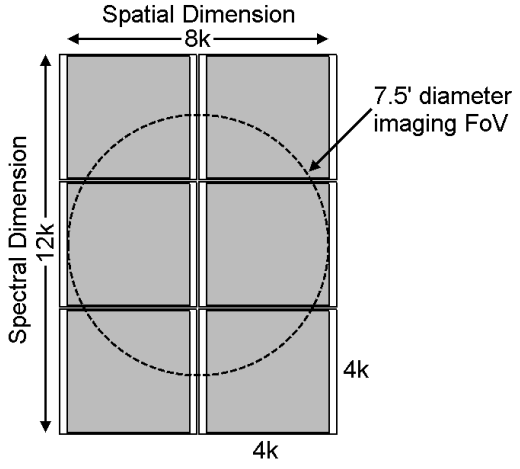

Figure 4. 12k-by-8k CCD mosaic forming the sensor assembly for the GMACS blue camera shown as shaded squares. The imaging FoV is shown by the dashed circle whose diameter is enclosed within the smaller sensor dimension. It is assumed that the dispersion direction is in the orthogonal dimension.

Table 3. Sensor Parameters

Unit Sensor	
Sensor	CCD type
Number of pixels (horizontal x vertical)	4096 x 4096
Sensor Size (horizontal x vertical)	61.44 mm x 61.44 mm
Full diagonal	86.89 mm
Pixel pitch (horizontal x vertical)	15 μm x 15 μm
Sensor Assembly	
CCD mosaic	2-by-3
Number of pixels (horizontal x vertical)	12288 x 8192
Sensor size (horizontal x vertical)	184.32 x 122.88mm

3.6 Beamsplitter & Filters

The beamsplitter is fused silica and will have a multi-layer dichroic coating on the first surface and anti-reflection coating on the second surface. A final determination for the split wavelength has not been made yet, but the nominal value is 557nm, the location of a strong atmospheric emission line. A final determination will be made considering observationally important spectral lines as well as practical constraints related to balancing the total spectrum between the two arms.

Order sorting filters are shown directly after the VPHG's in each arm. The bandpasses and number of filters will be determined as the design progresses. We are considering alternate locations, either fixed directly after the beamsplitter, or in front of the first element of the cameras. This will reduce the size of the filters and simplifies the mechanism for rotating and exchanging gratings.

3.7 VPH Gratings

The GMACS dispersive optics will be transmission Volume-Phase Holographic (VPH) Gratings. The spectral resolution requirement of 1000-6000 in both red and blue arms implies gratings with 660-2800 lines mm^{-1} for the blue arm and 400-2000 lines mm^{-1} in the red arm. The spectrograph will initially have three interchangeable gratings for each arm to accommodate both the lower resolution modes in which it will be possible to record complete spectra across the whole wavelength range of the instrument (350-950nm) in a single image as well as high resolution modes in which the simultaneous wavelength coverage will be sacrificed for higher resolution. The combination of adjustable collimator-camera angle and grating tilt will allow GMACS to "scan" across the entire spectral range in multiple snapshots.

Preliminary feasibility studies have been carried out to determine potential grating designs. The primary concerns are size, line density and grating efficiency. The required size is close to the upper limit of current manufacturing capabilities. The pupil sets the grating dimension in the spatial direction. The spectral dimension is set by the pupil size and the grating rotation required to satisfy the Bragg condition. For high resolutions this angle will approach 45° and elongate the required grating by a factor of $\sqrt{2}$. Fortunately, the method of producing the interference fringes used to generate the grating results in an elongated recording area, so that the diameter of the collimated laser beams used to record the fringes need only be as large as the smaller dimension (C. Clemens, private communication).

Line densities between 400 and 3000 lines mm^{-1} are well within the range of manufacturability and simulations of expected grating efficiencies predict excellent performance across the desired wavelength range. Two example grating efficiencies are shown in Figure 5, generated during the previous conceptual design study. At this time we do not anticipate a need to generate the large gratings in multiple stepped exposures.

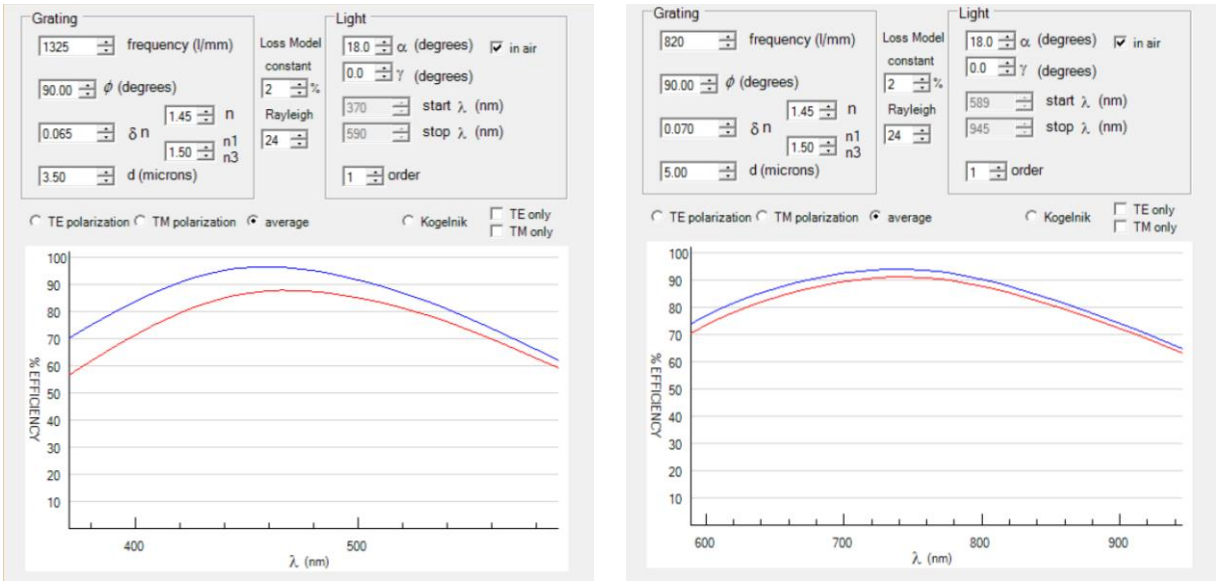

Figure 5. (Left) 1325 lines mm^{-1} blue grating (R~2300) with parameters as shown. The blue curve shows theoretical efficiency for 18 degree operating angle, and the red curve shows likely realized efficiency after surface and other grating losses. (Right) 820 lines mm^{-1} red grating (R~2300) with parameters as shown. The blue curve shows theoretical efficiency for 18 degree operating angle, and the red curve shows likely realized efficiency after surface and other grating losses.

4 GMACS OPERATION MODES

4.1 Imaging Mode

The GMACS image mode can be accomplished either through removal of the grating from the optical path, or potentially rotating the grating normal to the optical axis. The second option may be useful in determining target alignment with the slit mask. The basic parameters are summarized in the table below.

Table 4. Current blue camera imaging performance.

Optical performance:	
Full field of view	7.5 arcmin diameter
Image size	122mm diameter
Transmission	~46% across full field
Relative illumination (vignetting)	100% (no vignetting)
Encircled energy	RMS diameter ~43μm @ 7.5arcmin FoV
Distortion	< 1 %
Field curvature	< 0.7mm
Plate Scale	3.47 arcsec/mm

In spite of the relatively high field curvature and the longitudinal color, the effects in the spectroscopic mode may be mitigated by tilting the detector through a suitable mechanism determined by optical simulations.

The broad-band direct imaging is likely to be one of the least important modes for GMACS. Narrower band filter imaging may be accommodated through focus adjustment.

Shown below are GMACS in imaging mode and corresponding spot diagram for a 0.3 arcsec resolution. We will continue to optimize the design to meet the specifications in the next design phases, including tolerance and athermalization studies.

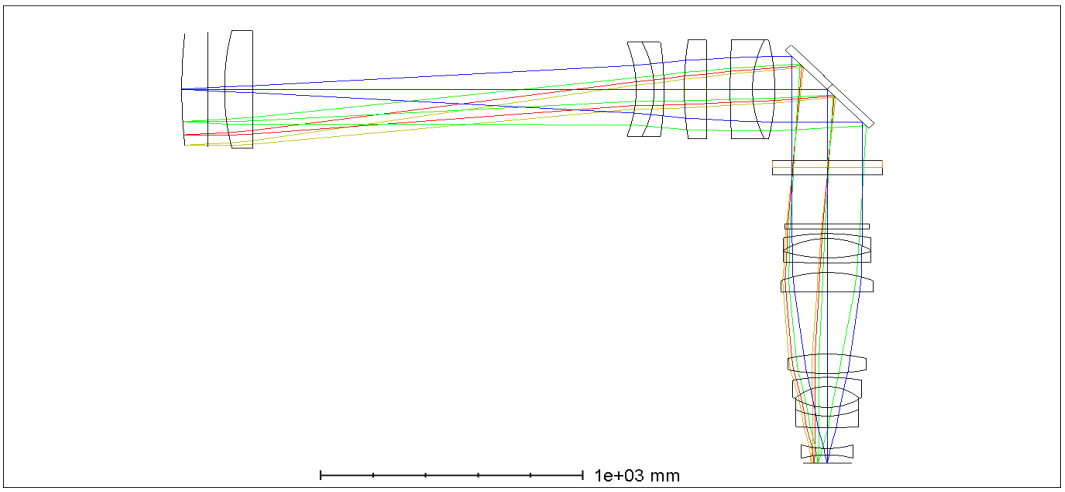

Figure 6. Imaging mode optical layout

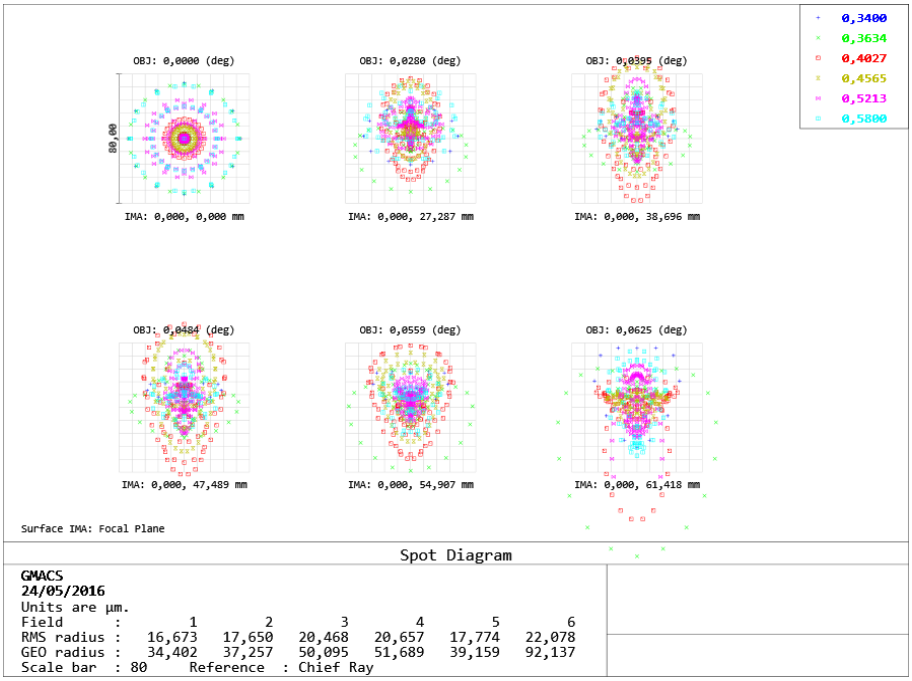

Figure 7. Spot Size Diagram, box is 0.3 arcsec on a side.

4.1.1 **Throughput analysis**

A throughput analysis of the GMACS optical system for imaging mode was performed. The throughput is mainly a function of the internal spectral transmittance of the glasses. Glass selection based on high transmittance in the UV-blue spectral range plays an important role in the overall design.

The telescope mirrors have an important influence on the system throughput. However, in this analysis, we considered only the influence of the collimator and camera, then we assume that a nominal 100% of energy is transmitted from the telescope focal plane

We included a quarter wave MgF_2 coating on all surfaces. Given that there is no vignetting in the image mode, the throughput can be considered constant as a function of FoV.

Figure 8 shows the throughput as a function of wavelength at the center of the FoV.

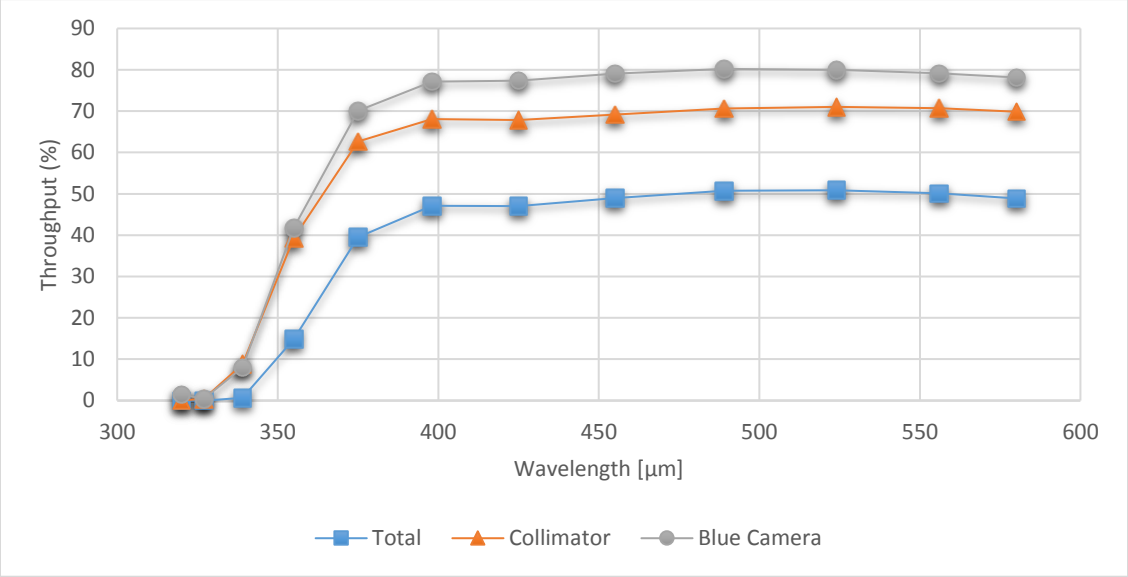

Figure 8. Image mode throughput for the collimator, camera and both as a function of wavelength for the central FoV

The normalized throughput at 350nm is about 13% of the maximum centered at 490nm and it is highly dependent on the thicknesses of the lenses of the glasses that present high absorption in blue-UV spectral region. A small thickness reduction during optimization or a glass replacement will have a strong effect on the UV throughput. It is noted that it is practically impossible to have a reasonable throughput at 320nm with a 10 element refractive camera.

4.2 Spectroscopic Mode

The low and medium resolution modes are still an ongoing optimization and the updated results are described in this section. The mechanical dimensions of the VPHG are determined by the elliptical footprint at its most extreme (45°) angle. Below is a table that shows the basic parameters for the slit and the plate scale generated by the telescope.

Table 5. Slit parameters

Slit width x length	0.7 arcsec x 7.4 arcmin 0.704 mm x 446.8 mm
Plate Scale at marked position	1 arcsec/mm

Below is the combined optical configurations layout for imaging, low and high resolution spectrograph modes.

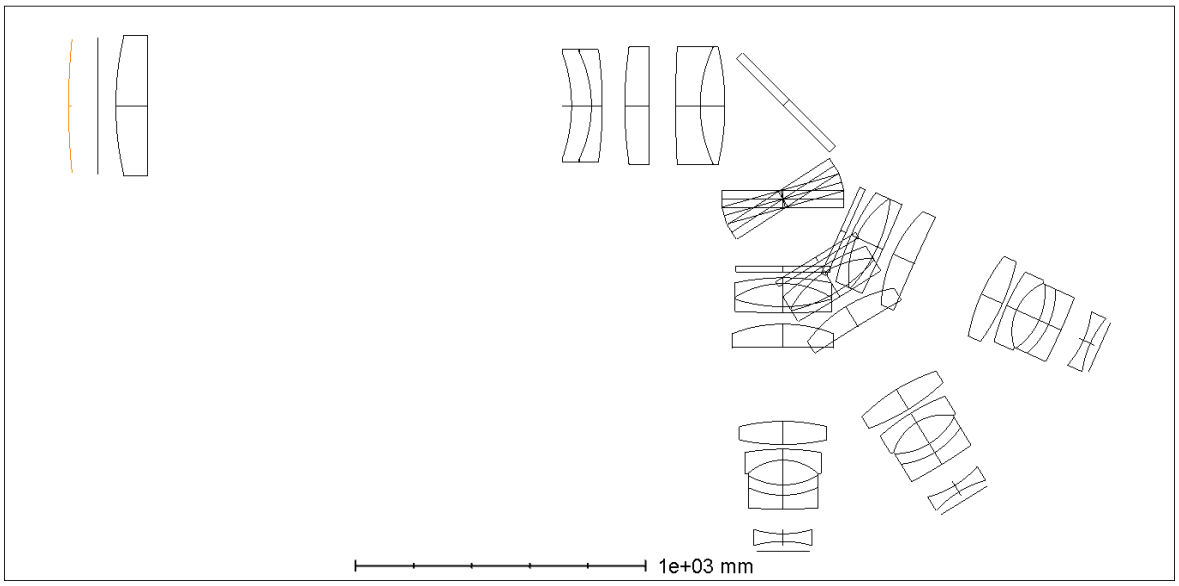

Figure 9. Optical layout showing the articulated camera in its imaging, low and high resolution modes for the blue camera case.

4.2.1 **Low resolution**

The basic parameters for the low resolution spectrograph mode are summarized in the Table below.

Table 6. Low resolution spectrograph performance

Anamorphic factor	1
Grating Lines/mm	1180
Diffraction Order	1
Center wavelength	480nm
Simultaneous wavelength coverage	253.05nm (Covering from 353.4 to 606.2nm)
Bragg angle	16.45°
Dispersion	0.0206nm/pixel
Pixel/slit width	12.6

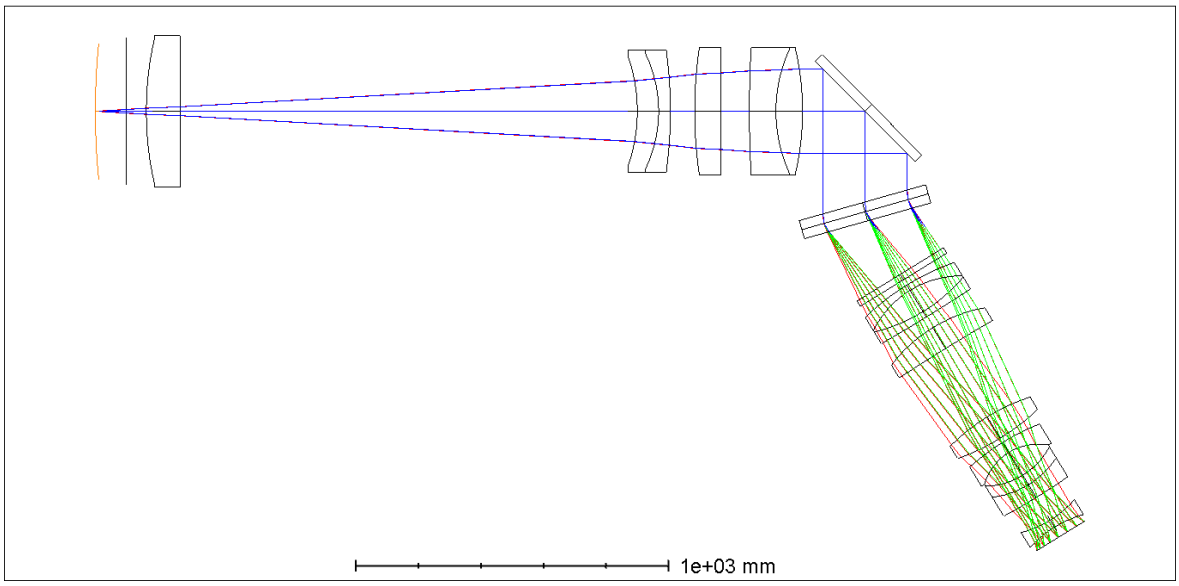

Figure 10. Example low resolution spectrograph layout for blue arm

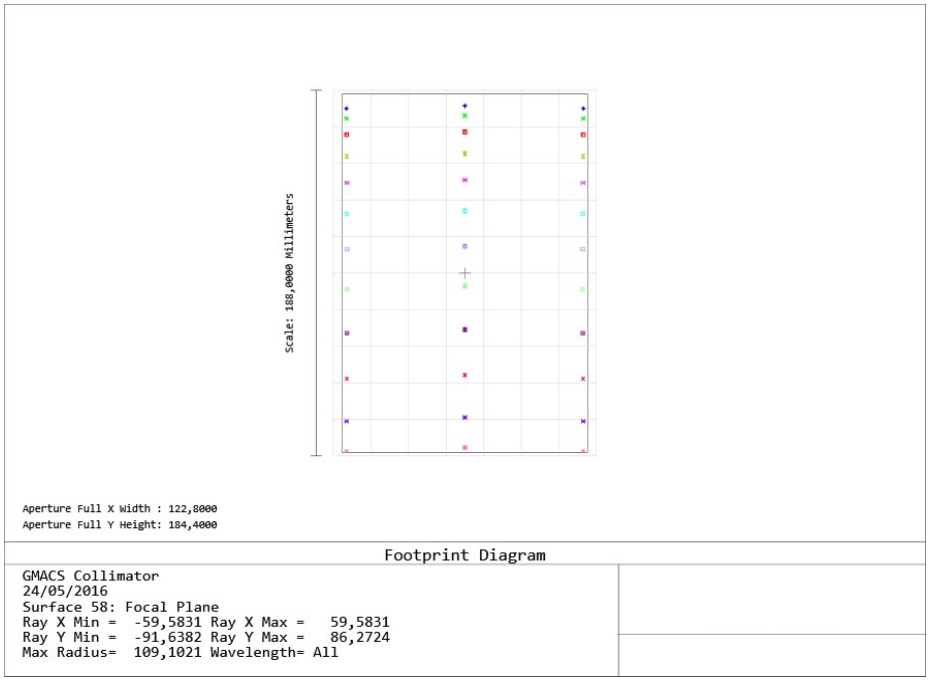

Figure 11. Footprint diagram for low resolution mode for 0.7 arcsec slit. The spectrum coverage shown in the image is from 340nm to 580nm (sampled top to bottom as follows: 340, 347, 359, 374, 393, 416, 441, 469, 500, 531, 560, 580nm).

The spot diagrams for the low resolution mode are presented in the image below:

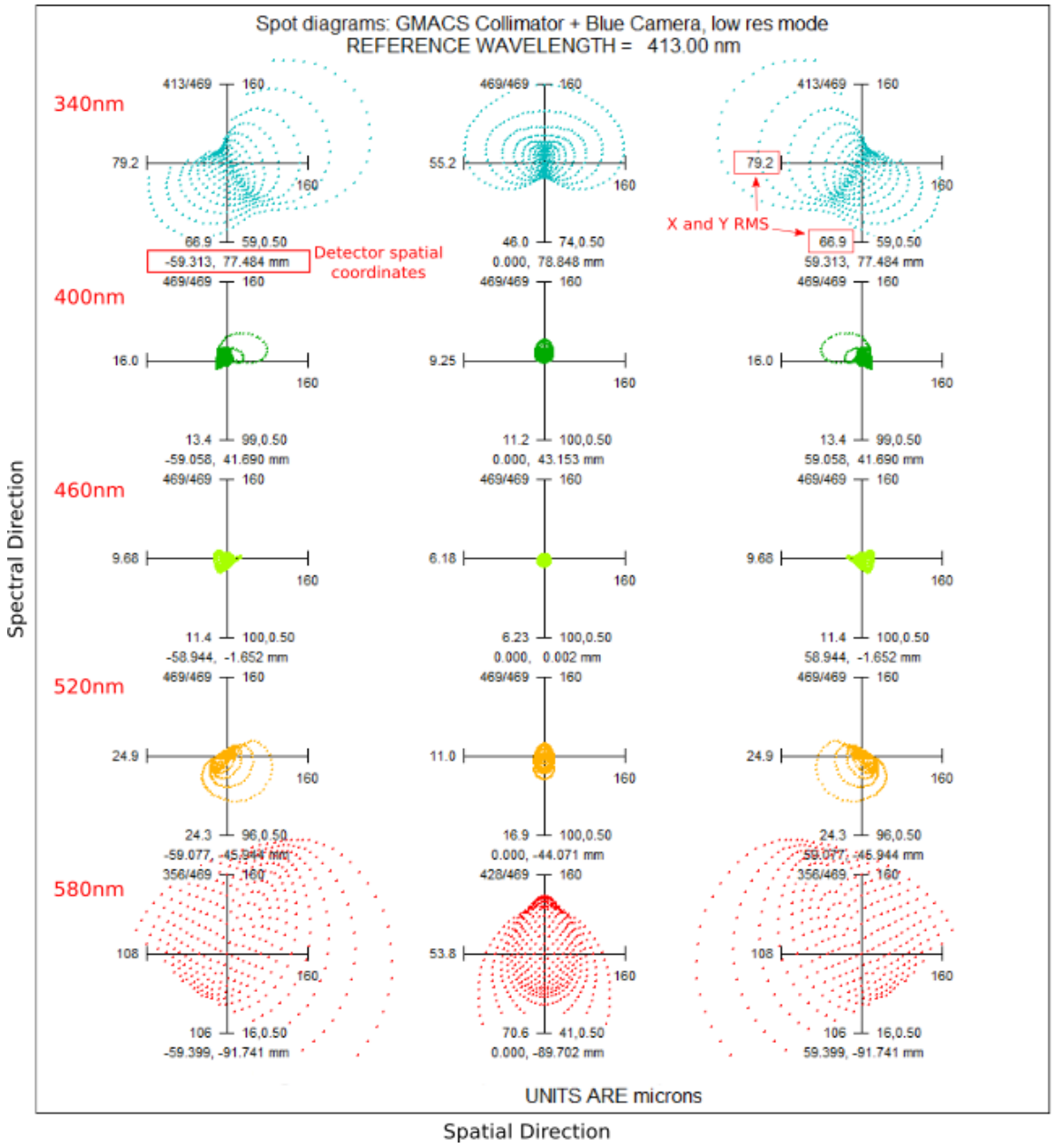

Figure 12. Spot diagram for low resolution mode from 340 to 580nm, sampled in the spectral dimension at: 340 (top), 400, 460, 520 and 580nm (bottom) with the spatial dimension sampled within a 2-by-3 mosaic of 4k² detectors. Each square has a size of 0.6 arcsec (160µm)

Although the RMS spot size for the low resolution spectrograph mode is acceptable for intermediate wavelengths, the spots at 340nm and 580nm give arguably unacceptably high values for RMS. The GMACS optical systems described in this paper were optimized only for imaging mode while the spectroscopic coverage was defined by the VPHG parameters. This means that no optimization was done specifically for the spectrographic modes. The next phase of the design process will include optimization of all spectrographic modes.

4.2.2 **High resolution**

The basic parameters for the high resolution spectrograph mode are summarized in the Table below.

Table 7. High resolution spectrograph performance

Anamorphic factor	1
Grating Lines/mm	2360
Diffraction Order	1
Center wavelength	480nm
Simultaneous wavelength coverage	108.73nm (from 425.64 to 534.36nm)
Bragg angle	34.5°
Dispersion	0.0088nm/pixel
Pixel/slit width	12.6

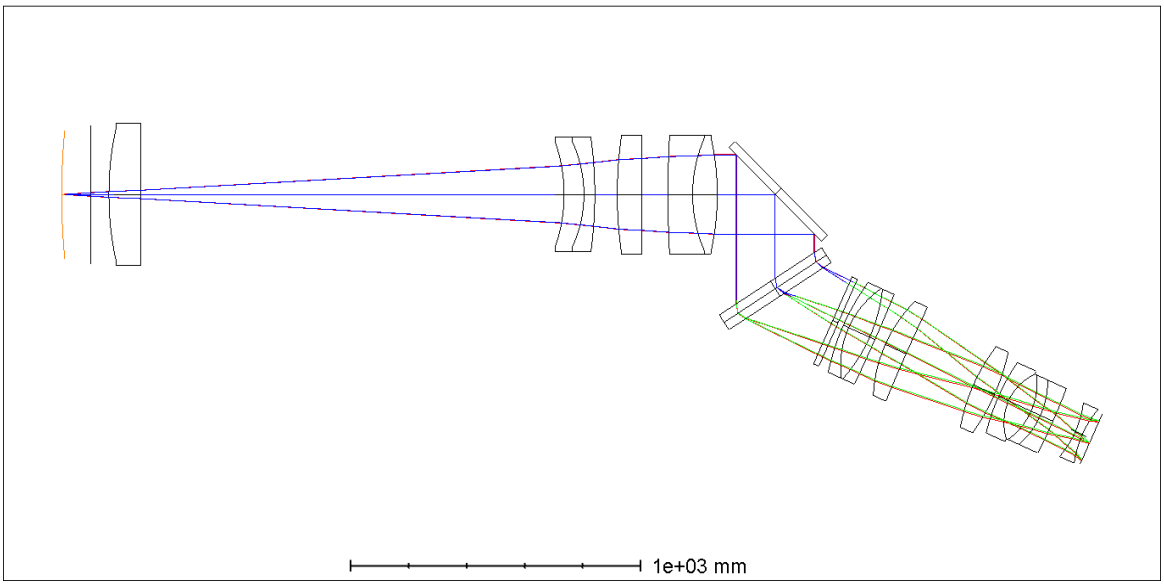

Figure 13. High resolution spectrograph layout for blue arm

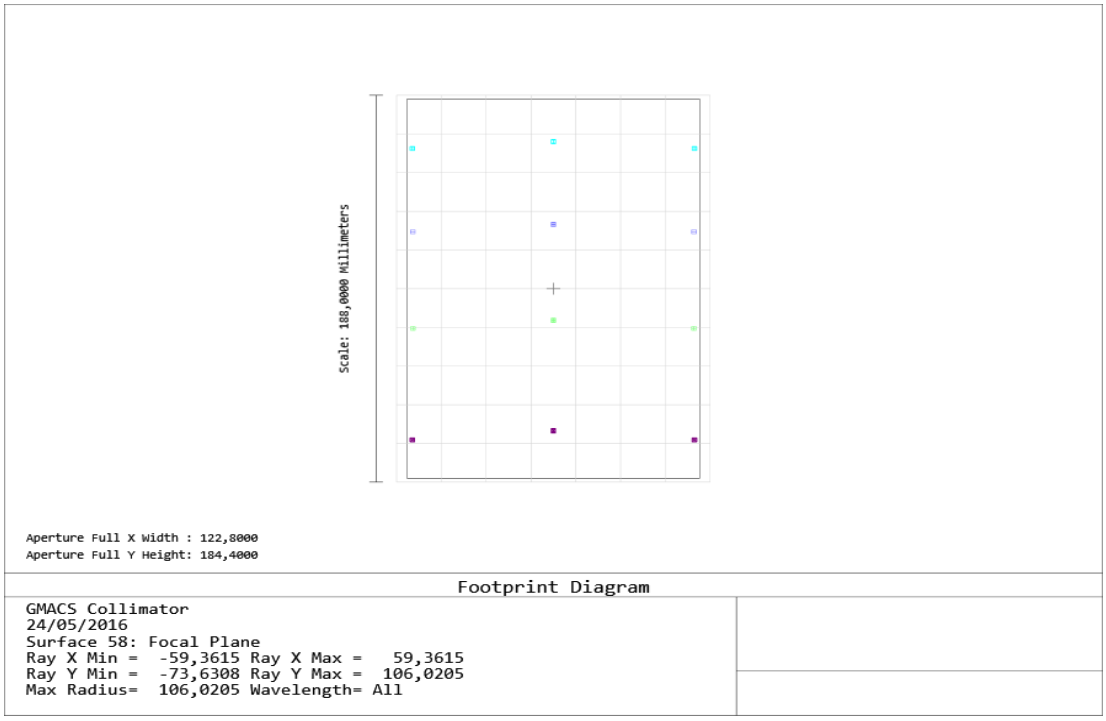

Figure 14. Footprint diagram for high resolution mode for a 0.7 arcsec slit. The spectrum coverage shown in the image is from 416 to 500nm. It is possible to see the characteristic curvature along the spatial space

As an on-going project, we are studying a larger range of dispersions encompassing intermediate and the highest dispersion modes. A currently unresolved issue has to do with mechanical restrictions to the camera articulation. If such modes are permitted it will be possible to reach resolutions approaching R~10,000.

5 GLASS SELECTION

The internal transmittance of the materials and the availability of required thicknesses and diameters of blanks from optical glass suppliers are major concerns for the collimator and blue camera optical design. The appropriate selection of glasses has a significant impact on the throughput of the system, especially in the UV.

In addition to the diameter restriction of the selected glasses, the requirement of the instrument for high transmittance in the extreme UV (<340nm) dramatically decreases the number of options.

5.1 Methodology

The methodology for glasses selection is based on the optical suppliers' reported capabilities to produce blanks with the dimensions and quality required for the GMACS design. Given the requirement for blank diameters larger than ~300mm, thickness larger than ~40mm having a minimum of ~80% internal transmittance in the 320 to 340nm spectral range, the following glasses were identified as potential candidates: CaF2, Fused Silica, BAL35Y, FSL5, BSL7Y, BSM51Y, BAL35Y, FPL51Y, NIGS4786, PSK3, FK54. (The choice of glasses for the red camera is less restrictive and so material availability will not be as critical as it is for the blue camera design.)

The effort to improve glass availability which meets the demands of the GMACS optical system is an on-going process involving discussions with potential suppliers.

5.2 Differential Abbé Number for apochromatism

We have noticed that current GMACS optical designs suffer from strong chromatic aberrations, such as sphero-chromatism and other high-order chromatic effects that limit the performance of the system. However, these effects can be satisfactorily corrected by the use of an effective method for comparing the dispersive properties of optical glasses so as to minimize high order chromatic effects. The method is described in detail by Jones 2014[6].

The motivation for this technique was driven by the "patchiness" of catalogued "Relative Partial Dispersion" data, the crudeness of their calculation and the observation that the "Abbe V-number" for a particular glass is a strong function of the chosen wavelength interval.

The main idea is to combine the condition of longitudinal achromatism in a system with the differential V-numbers, centered in a wavelength λ, defined by

$$dV_i = \frac{n(\lambda_i) - 1}{-\frac{\delta n(\lambda_i)}{\delta \lambda}} \tag{1}$$

Where n is the index of refraction. The minus sign in the denominator is there to keep dV positive.

The classical solution for apochromatism in a multi-glass system (for example, a doublet) demands that the relative partial dispersions of the different glasses be as close as possible. It is shown in Jones 2014[6] that we can define a differential quantity:

$$dRPD_i = \frac{dV_{i-1}}{dV_i} \tag{2}$$

Where dRPD is a "differential Relative Partial Dispersion". Glasses can now be selected based on maximizing the differences in dV while minimizing differences in dRPD. The utility of this method is that the dispersive relationships between glasses can be simply demonstrated. As an example, Figure 15 plots dV and dRPD curves for some catalogue glasses over an "extended-visible" waveband, for a δλ of 5nm.

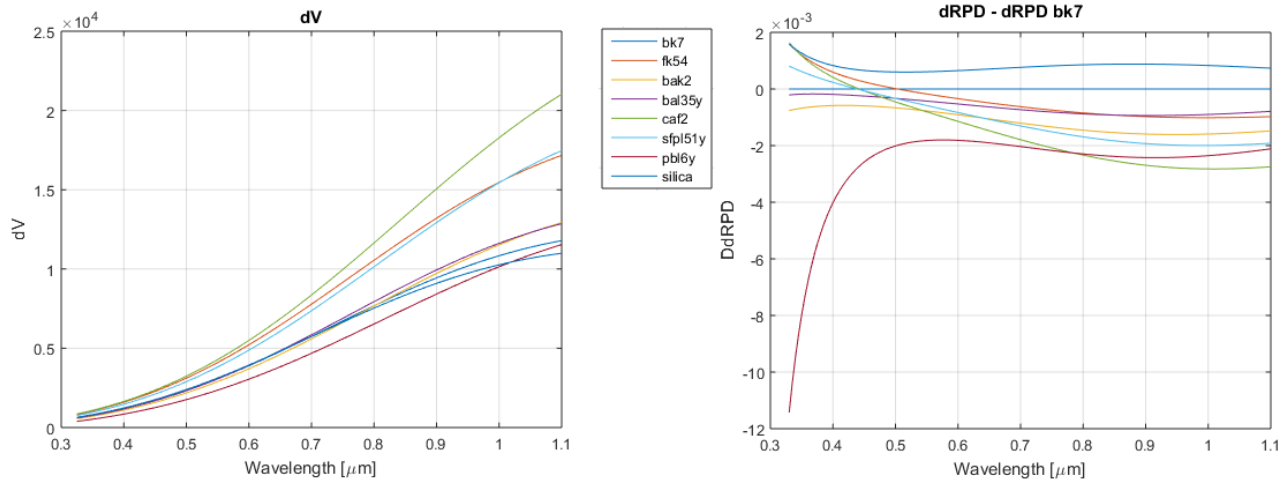

Figure 15. dV and dRPD for a selection of catalogue glasses over the "extended visible" waveband.

We note that the dV curves for the selected glasses fall to nearly zero towards the short wavelength end of the band. Although the curves are falling in more or less constant proportion with roughly matching dRPD properties the dispersive strengths of the individual glasses are increasing rapidly. The consequence of this is that colour correction into the UV becomes increasingly problematic. This will be explored as the optical design proceeds. The dRPD method briefly described above was used as a guide in this work for the determination of the best combination for the collimator and camera glasses to avoid chromatic effects.

6 AUXILIARY SYSTEMS

6.1 Guide and Acquisition Cameras

In order to position target objects on their respective slits, a guide and acquisition system will be necessary. This system will consist of cameras placed at the edge of the spectrograph mask, each having approximately a 1 arcminute FoV. Three of the cameras will be fixed and a fourth camera with a smaller FoV will be capable of moving around the spectrograph field under the mask to confirm target object placement on the slits. The curved focal plane and lack of a wide field corrector will require a small off-axis corrector for each fixed acquisition camera. This system will be valuable during the commissioning of GMACS, and as errors in telescope pointing and telescope-instrument flexure are better understood we expect reduced need for the movable camera. The acquisition cameras will likely be doublet or triplet lenses and are in very early stages of design. The location of the cameras is shown in Figure 16.

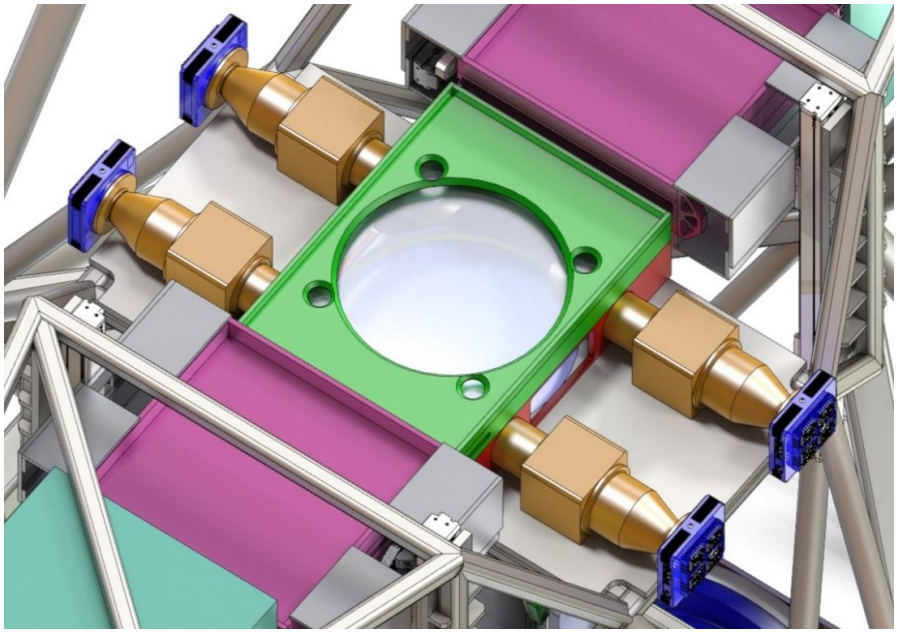

Figure 16. Top down view of the slit mask location, which also shows four off-axis guide and acquisition cameras.

6.2 Flexure Compensation

GMACS is mounted at the Gregorian focus position of the GMT and therefore experiences a constantly changing orientation as the telescope tracks an object across the sky. In order to meet the requirement for spectral stability of 0.3 spectral resolution elements per hour, the gravity-induced flexure of the instrument must be tracked and compensated. Eventual integration with MANIFEST and the resulting smaller slit sizes will require even stricter flexure compensation requirements. The reconfigurable nature of GMACS (many possible camera-collimator angles) will make a look-up table based compensation system intractable. Therefore we plan to develop a closed-loop system that will track the motion of set reference points within the instrument. One such system could use lasers and quad-cells placed to measure relative motion between fiducial points[7,8,9]. The current concept mounts each camera within a hexapod which will allow a full six degrees of freedom for correction at the focal plane. A robust tolerance analysis will be critical in defining the performance requirements of the flexure compensation system.

6.3 MANIFEST

Integration with MANIFEST will increase the multiplexing capabilities of GMACS and extend its FoV to the full GMT 20 arcminute diameter field. We have investigated several possible locations for the MANIFEST feed optics. At this time we intend to replace the mask at the telescope focal plane with the fiber outputs from MANIFEST. As this will require no additional or exchangeable GMACS optics, it only impacts the optical performance and flexure control requirements for GMACS. Collaboration with the MANIFEST team has been initiated and we expect both teams to continue development in tandem. Progress with MANIFEST development is given in paper 9908-358[10] at this conference.

7 FUTURE WORK

In this section we describe some of the future work we will perform in parallel to the optical design optimization.

Our first trade study will concern developing faster cameras which will yield larger FOV's. The focal distances of the collimator and the camera, FoV and detector size are interdependent parameters which can be modified based on several project requirements and restrictions. We have chosen to start the design process with the optical parameters listed in Table 2 to demonstrate the viability of the proposed GMACS optical system. However, different configurations can be chosen to reach different performance goals, for instance higher FoV, or a reduction in the number of detectors in each array.

We also plan to explore an observing mode in which the camera is rotated about the optical axis by 90°. This implementation of a camera rotation mechanism would allow a swap between the dispersion and slit direction at the detector when spatial, rather than spectral, coverage is at a premium. This feature would add to the optomechanical complexity and require significant field widening of the collimator, both of which have yet to be explored.

Finally, we will explore a catadioptric ~*f*/1 solution with a 4k-by-6k detector for the UV/blue arm, where internal detector vignetting losses are less than transmission losses. The most difficult requirement for the blue camera design is the 25% of peak throughput at the UV bandpass limit. To accomplish this a careful glass selection must be performed based not only on supplier's capabilities, but the glasses' internal transmittance. These restrictions result in very limited glass choices suitable for design and optimization. Therefore, in order to provide an alternative to avoid the restriction of the internal transmittance of the glasses, we are studying the possibility and desirability of designing an ~*f*/1 catadioptric camera with a unique 4k x 6k detector only for the blue camera. Although this camera concept causes throughput losses due to the obscuration, the effective throughput would not be as highly dependent on the wavelength as it is for the refractive camera. The refractive elements of the catadioptric camera, for instance, the flattener lens/subsystem, can be manufactured with high internal UV transmittance glasses (fused silica and CaF_2). This catadioptric camera concept can considerably increase the UV throughput.

8 ACKNOWLEDGEMENTS

Texas A&M University thanks Charles R. '62 and Judith G. Munnerlyn, George P. '40 and Cynthia Woods Mitchell, and their families for support of astronomical instrumentation activities in the Department of Physics and Astronomy. The authors would also like to thank C. Clemens for helpful discussions on VPH gratings and efficiency modeling.

REFERENCES

[1] DePoy, D. L., Allen, R., Barkhouser, R., Boster, E., Carona, D., Harding, A., Hammond, R., Marshall, J. L., Orndorff, J., Papovich, C., Prochaska, K., Prochaska, T., Rheault, J. P., Smee, S., Shectman, S., Villanueva, S., "GMACS: a wide field, multi-object, moderate-resolution, optical spectrograph for the Giant Magellan Telescope," Proc. SPIE 8446, Ground-based and Airborne Instrumentation for Astronomy IV, 84461N (2012).

[2] DePoy, D. L., Marshall, J. L., Cook, E., Froning, C. S., Ji, T., Jones, D. J., Lee, H., Mendes de Oliveira, C., Pak, S., Papovich, C., Prochaska, T., Ribeiro, R., Schmidt, L. M., Taylor, K., "The Giant Magellan Telescope multi-object astronomical and cosmological spectrograph (GMACS)," Proc. SPIE 9908, Ground-based and Airborne Instrumentation for Astronomy VI, 990879 (2016).

[3] Prochaska, T., Schmidt, L. M., Ribeiro, R., DePoy, D. L., Marshall, J. L., Cook, E., Froning, C. S., Taylor, K., Jones, D. J., Pak, S., Ji, T., Lee, H., Mendes de Oliveira, C., Papovich, C., "Optomechanical design concept for the

Giant Magellan Telescope Multi-object Astronomical and Cosmological Spectrograph (GMACS),” Proc. SPIE 9908, Ground-based and Airborne Instrumentation for Astronomy VI, 9908375 (2016).

[4] Lawrence, J. S. , Brown, D. M., Brzeski, J., Case, S., Colless, M. Farrell, T., Gers, L., Gilbert, J., Goodwin, M., Jacoby, G., Hopkins, A. M., Ireland, M., Kuehn, K., Lorente, N. P. F., Miziarski, S., Muller, R., Nichani, V., Rakman, A., Richards, S., Saunders, W., Staszak, N. F., Tims, J., Vuong, M., Waller, L., "The MANIFEST fibre positioning system for the Giant Magellan Telescope," Proc. SPIE 9147, Ground-based and Airborne Instrumentation for Astronomy V, 914794 (2014).

[5] Smith, W. J., [Modern Lens Design: a Resource Manual], McGraw-Hill Professional, New York NY, 488-489 (1992).

[6] Jones, D. J., “A Glass Selection Method for Apochromatism: introducing the differential Abbé number,” PrimeOptics, 29 September 2014, <http://www.primeoptics.com.au/Reference/dRPD_description.pdf> (30 May 2016).

[7] Marshall, J. L., Atwood, B., Byard, P. L., DePoy, D. L., O'Brien, T. P., Pogge, R. W., "An Image Motion Compensation System for the Multi-Object Double Spectrograph," Proc. SPIE 4841, Instrument Design and Performance for Optical/Infrared Ground-based Telescopes, 1273 (2003).

[8] Marshall, J. L., Atwood, B., Byard, P. L., DePoy, D. L., O'Brien, T. P., Pogge, R. W., "An Image Motion Compensation System for the Multi-Object Double Spectrograph," Proc. SPIE 5492, Ground-based Instrumentation for Astronomy, 739 (2004).

[9] Marshall, J. L. , O'Brien, T. P., Atwood, B., Byard, P. L., DePoy, D. L., Derwent, M., Eastman, J. D., Gonzalez, R., Pappalardo, D. P., Pogge, R. W., "An image motion compensation system for the multi-object double spectrograph," Proc. SPIE 6269, Ground-based and Airborne Instrumentation for Astronomy, 62691J (2006).

[10] Lawrence, J. S. , Brown, D. M., Brown, R. A., Case, S., Chapman, S., Churilov, V., Colless, M. M., Content, R., Goodwin, M., Klauser, U., Kuehn, K., Lorente, N. P. F., Mali, S., Muller, R., Nichani, V., Pai, N., Saunders, W., Shortridge, K., Staszak, N. F., Tims, J., Vuong, M., Waller, L. G., Zhelem, R., “The MANIFEST prototyping design study,” Proc. SPIE 9908, Ground-based and Airborne Instrumentation for Astronomy VI, 9908358 (2016).